

4. "News Item," *Chem. Eng.* (March 5, 1962).
5. Emmett, P. H., Ed. "Catalysis," Vol. VII, p. 183, Reinhold, New York (1960).
6. Fair, J. R., J. W. Mayers, and W. H. Lane, *Chem. Eng. Progr.*, **53**, 433 (1957).
7. Gorin, Everett, C. M. Fontana, and Kidder, G. A., *Ind. Eng. Chem.*, **40**, 2128 (1948).
8. Hanmer, R. S., and Sherlock Swann, Jr., *Ind. Eng. Chem.*, **41**, 325 (1949).
9. Johnson, P. C., and Sherlock Swann, Jr., *ibid.*, **38**, 990 (1946).
10. Leibnitz, E., H. G. Konnecke, and H. Knopel, *J. Praktische Chem.*, **4**, 298 (1957).
11. Levich, U. G., "Physicochemical Hydrodynamics," p. 395, Prentice-Hall, Englewood Cliffs, N. J. (1962).
12. Loftus, Jordan, Sc.D. thesis, Massachusetts Inst. Technol., Cambridge (1963).
13. ———, and C. N. Satterfield, *J. Phys. Chem.*, **69**, 909 (1965).
14. Nonnenmacher, H., M. Appl, and K. Andrusson. German patent 1, 144,709, assigned to Badische Anilin & Soda Fabrik (March 6, 1963).
15. Parks, W. G., and C. E. Allard, *Ind. Eng. Chem.*, **31**, 1162 (1939).
16. *Petrol. Refiner*, **42**, No. 11, 210 (1963).
17. Satterfield, C. N., and Jordan Loftus, *Ind. Eng. Chem. Process Design Develop.*, **4**, 102 (1965).
18. Simard, G. L., J. F. Steger, R. J. Arnott, and L. A. Siegel, *Ind. Eng. Chem.*, **47**, 1424 (1955).
19. Sundmeyer, W., O. Glemser, and K. Kleine-Weischede, *Chem. Ber.*, **95**, 1829 (1962).
20. Tøpsøe, H. F. A., and Anders Nielsen, *Trans. Dan. Acad. Tech. Sci.*, **1**, 18 (1948).
21. Tribin, H. C., Jordan Loftus, and C. N. Satterfield, submitted for publication.

*Manuscript received March 25, 1965; revision received July 10, 1965; paper accepted July 26, 1965. Paper presented at A.I.Ch.E. Boston meeting.*

# The Determination of Eddy Mass Diffusivities for the Air-Water System in a Wetted-Wall Column

DAVID W. BUNCH and MAILAND R. STRUNK

University of Missouri, Rolla, Missouri

Eddy mass diffusivities as a function of radial position for different Reynolds numbers have been determined for air flowing countercurrently to water in a wetted-wall column. The ratios of the eddy mass diffusivity to the eddy viscosity also were determined. The wetted-wall column was constructed from Pyrex glass with an I.D. of 2.75 in. and a wetted section 39 in. in length. An approach section was constructed from the same material and of adequate length to insure full development of the velocity profile. The gas phase Reynolds numbers varied from 3,200 to 54,300. The liquid phase flow was laminar. The concentration and velocity profiles of the air stream were measured experimentally and bulk temperatures of all streams were obtained. A probe was developed to measure the concentration profiles. The probe consisted of platinum wires wrapped in a helix around a glass capillary tube on which a thin layer of lithium chloride in polyvinyl alcohol had been deposited. The resistance of the probe was a reliable indication of the water vapor concentration in the air stream. The probe was calibrated and used for all concentration measurements. Eddy mass diffusivities were evaluated from a solution of the steady state mass diffusion equation by means of a digital computer with experimental velocity and concentration profiles. Qualitatively, the eddy diffusivity profiles are similar to those which have been obtained for heat and momentum transfer. When these profiles are used with the diffusion expression, they are capable of accurate evaluation of the concentration profile. The ratio of the eddy mass diffusivity to the eddy viscosity was determined and was found to be less than 1.0 over most of the cross section, but the ratio increased to values greater than 1.0 near the center and near the walls of the column.

Boussinesq (1) has suggested that the eddy diffusivity be defined in a manner analogous to the molecular diffusivity; that is

$$\frac{N_a}{A} = -E \frac{dc_a}{dx} \quad (1)$$

A combination of the molecular and eddy effects leads to the general expression for the total mass transferred

David W. Bunch is with Ethyl Corporation, Baton Rouge, Louisiana.

$$\frac{N_a}{A} = -(D_e + E) \frac{dc_a}{dx} \quad (2)$$

Various investigators have found (2 to 4) that the eddy diffusivity varies with position; that is

$$E = E(x) \quad (3)$$

Tao and Strunk (5) recently determined eddy thermal diffusivities for air flowing in circular conduits at various

radial positions for different Reynolds numbers. In reference 5 values of the eddy thermal diffusivity, eddy viscosity, and ratio of eddy thermal diffusivity to eddy viscosity for numerous radial positions were evaluated. The purpose of this investigation was to determine the eddy mass diffusivities for the air-water system at various radial positions for different Reynolds numbers. A comparison of these values with those from heat transfer measurements could then be made. There is a scarcity of such experimental data in the literature.

The wetted-wall column has been used by a number of investigators. Gilliland and Sherwood (6) used such a column to study the evaporation of several different liquids into turbulent air streams. McCarter and Stutzman (7) used a wetted-wall column to investigate the diffusion of several different liquids into air. Schwartz and Hoelscher (4) conducted studies in a wetted-wall column and obtained local values of the eddy mass and momentum diffusivities as well as the local mass transfer rates for water evaporating into air. All their observations were at a Reynolds number of 25,000. Their concentrations were determined at various radial positions by withdrawing air samples, and then passing them through tubes containing commercial Drierite which were then weighed.

Also of interest are the works of Johnstone and Pigford (8) and that of Surowiec and Furnas (9) who studied rectification in wetted-wall columns. Jackson (10) and Thomas and Portalski (11, 12) conducted extensive hydrodynamic studies on wetted-wall columns and established limits on the extent of the laminar zone for the flow of the liquid phase.

In a recent study of the effect of liquid flow properties on mass transfer, Kafesjian, Plank, and Gerhard (13) studied the effects of rippling in the liquid phase. They found that for a liquid phase Reynolds number less than 25, the flow of liquid is nonrippling. In this present work the flow of water down the column was maintained in the laminar region at all times to minimize rippling effects.

Several investigators, including the authors, have used surface active agents to reduce rippling. Among these have been Schwarz and Hoelscher (4), Jackson (10), and Emmert and Pigford (14). Emmert and Pigford determined that the addition of a wetting agent has little effect upon the assumed boundary condition at the interface. Schrage (15), using the data of Gilliland and Sherwood (6), also showed the interfacial resistance due to a wetting agent to be negligible.

## EXPERIMENTAL EQUIPMENT

A glass column similar in most features to that used by other investigators was used. The column was constructed from Pyrex glass with an I.D. of 2.75 in. An approach section was constructed of the same material to insure development of the velocity profile. Air was passed upward through the column countercurrent to a film of water which flowed down the inside perimeter of the column. The column exhausted into open air at the top. The wetted length of the column was 39 in.

The water phase contained a small amount of a commercial liquid detergent to prevent rippling of the liquid surface. The condition of the liquid surface was observed by viewing down the column as well as by viewing laterally to assure that complete wetting was attained at all times. Although the liquid phase Reynolds number ( $4r/\mu_L$ ) varied from 120 to 180 in the laminar region, this was considerably above 25 which is the upper limit for nonrippling. The amount of detergent used was less than 0.1% of the total liquid in the system. As the introduction of this small quantity of detergent created a foaming problem in some sections of the recirculation system, it was necessary to add a few drops of a foam suppressant. The addition of these foreign substances lowered the vapor pressure by a slight amount. The actual vapor pressures of

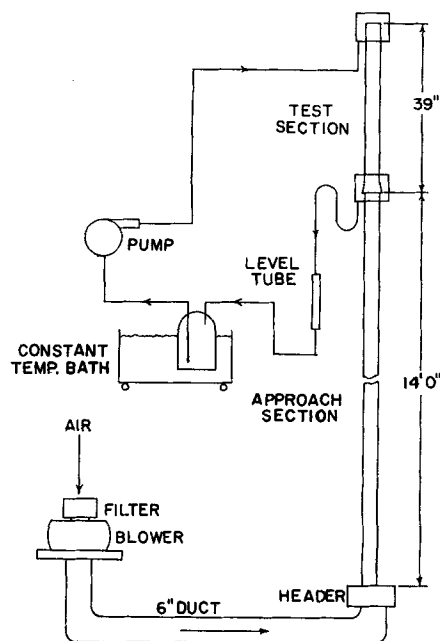


Fig. 1. Schematic diagram of experimental apparatus.

the water used in the system were incorporated in the calculations. The gas phase Reynolds number varied from 3,200 to 54,300. A schematic diagram of the apparatus is presented in Figure 1.

A small probe was constructed to measure the concentration profiles. The probe consisted of platinum wires wrapped in a helix around a glass capillary tube on which a thin layer of lithium chloride in polyvinyl alcohol had been deposited. The probe was slightly less than 2 mm. in diameter and 3 in. in length. The lithium chloride and wires were placed on only the lower portion of the tube. Strunk, Mitrovic, and Bunch (16) previously discussed such a probe and demonstrated its usefulness and accuracy. The resistance of the probe was found to be a reliable indication of the water vapor concentration in a gas at that particular location. The probe was calibrated and used for all concentration measurements. The concentration profiles integrated over the cross-sectional area were consistent with the bulk properties such as the mass transfer coefficient and the actual water evaporation rate.

Velocity profiles were obtained by measuring the velocity head with a carefully made impact tube constructed from a hypodermic needle having a diameter of approximately 0.02 in. The pressure measurements were determined by means of an ultrasensitive micromanometer which was capable of indicating a differential pressure of 0.001 in. of water.

A traversing mechanism was constructed from aluminum to provide a movable base for the velocity and concentration probes. This mechanism was mounted at the top of the column in such a way that the sensing elements were located 38 in. above the bottom of the wetted-wall section. The traversing mechanism was so constructed that the concentration or velocity probe could be positioned and advanced radially by means of a micrometer mechanism. The distance traveled was read on a micrometer barrel which had 0.001 in. as its smallest reading.

## EVALUATION OF THE EDDY FUNCTION

The appropriate expression for mass transfer in cylindrical coordinates under steady state conditions in terms of the partial pressure is

$$u(r) \frac{\partial P_a}{\partial z} = \frac{1}{r} \frac{\partial}{\partial r} \left[ r D_{ab} \frac{\partial P_a}{\partial r} \right] \quad (4)$$

In Equation (4) the physical properties of the fluids are assumed constant, axial diffusion is negligible, the velocity

is a function of radial position only, and both velocity and concentration profiles are symmetrical about the centers. The boundary conditions describing the system are

- B.C. 1 at  $r = R$ ,  $P_a = P_a^o$   
 B.C. 2 at  $z = 0$ ,  $P_a = P_i$   
 B.C. 3 at  $r = 0$ ,  $(\partial P_a)/(\partial r) = 0$

It should be noted that equilibrium is assumed to exist at the interface. The diffusivity term  $D_{ab}$  may be interpreted as a combination of the molecular and eddy diffusivity, that is

$$D_{ab} = D_c + E(r) \quad (5)$$

Equation (4), expressed in dimensionless form, becomes

$$U(X) \frac{\partial \theta}{\partial Z} = \frac{2}{X} \left[ B \frac{\partial \theta}{\partial X} + X \frac{\partial B}{\partial X} \frac{\partial \theta}{\partial X} + XB \frac{\partial^2 \theta}{\partial X^2} \right] \quad (6)$$

The transformed boundary conditions are

- B.C. 1 at  $X = 1$ ,  $\theta = 0$   
 B.C. 2 at  $Z = 0$ ,  $\theta = 1$   
 B.C. 3 at  $X = 0$ ,  $(\partial \theta)/(\partial X) = 0$

In this dimensionless form, Equation (6) is identical in form to the expression for heat transfer with constant wall temperature. The solution, using the method of separation of variables, yields an expression containing eigenvalues and eigenfunctions as follows:

$$\theta(X, Z) = \sum_{n=0}^{\infty} C_n R_n(X) e^{-\lambda_n^2 Z} \quad (7)$$

where  $R_n$  is a solution of

$$\frac{d}{dX} [XBR_n'(X)] + \frac{1}{2} \lambda_n^2 U(X)XR_n(X) = 0 \quad (8)$$

with boundary conditions

- B.C. 1A  $R_n(0) = 1$   
 B.C. 2A  $R_n(1) = 0$   
 B.C. 3A  $R_n'(0) = 0$

Equation (8) is a Sturm-Liouville type of differential equation. The eigenfunctions  $R_n(X)$  are orthogonal with respect to the weighting function  $1/2 XU(X)$  in the interval from 0 to 1.

If it can be assumed in Equation (7) that only the first term in the infinite series is significant, Equation (7) becomes

$$\theta(X, Z) = C_1 R_1(X) e^{-\lambda_1^2 Z} \quad (9)$$

At  $X = 0$ , Equation (9) becomes

$$\theta(0, Z) = C_1 R_1(0) e^{-\lambda_1^2 Z} \quad (10)$$

But from B.C. 1A

$$R(0) = 1$$

Thus

$$C_1 = \theta(0, Z) e^{\lambda_1^2 Z} \quad (11)$$

Substitution of  $C_1$  into Equation (9) gives

$$R_1(X) = \theta[X, Z]/\theta[0, Z] \quad (12)$$

Therefore, the first eigenfunction can be approximated as the ratio of the dimensionless concentration at any radial position to that at the center.

From the orthogonal properties of the eigenfunctions,  $C_n$  may be determined as

$$C_n = \frac{\int_0^1 U(X)XR_n(X)dX}{\int_0^1 U(X)XR_n^2(X)dX} \quad (13)$$

Then the constant  $C_1$  of Equation (9) may be evaluated from numerical integration of the experimental velocity data and eigenfunctions by using Equation (13). The eigenvalue  $\lambda_1^2$  may then be found by rearrangement of Equation (11)

$$\lambda_1^2 = \frac{1}{Z} \ln \left[ \frac{C_1}{\theta(0, Z)} \right] \quad (14)$$

Integration of Equation (8) then yields the eddy function

$$B(X) = \frac{-\lambda_1^2}{2XR_1'(X)} \int_0^1 XU(X)R_1(X)dX \quad (15)$$

At this point the entire calculation can be reversed and the concentration profile computed and compared with the experimental profile if a knowledge of the eddy function and the velocity profile is known.

Strunk and Tao (17) presented a numerical method for solving such a problem whereby the eigenvalue and eigenfunctions can be determined. The concentration profile can then be calculated from Equation (7). This provides a check on the validity of the eddy diffusivity function. In most cases, the regenerated eigenfunction failed to fulfill the boundary requirement at  $X = 1$

$$R_n(X) = 0$$

However, by adjusting slightly the value of  $B(0.95)$ , the eigenfunction could be forced to meet the boundary condition. The justification for making this slight adjustment for  $B(0.95)$  was due to the difficulty of obtaining accurate concentration measurements in the immediate vicinity of the wall. This difficulty arises because of the following reasons:

1. Near the wall, the presence of the concentration measuring device tends to disturb the liquid phase flow. This was observed visually during the experiments.
2. The possibility of entrained droplets on the concentration probe is greater in the region near the liquid surface.
3. The slope of the concentration distribution at the wall is very steep. Thus, a small error in the positioning of the probe could result in a large error in the concentration.

The evaluation of the eddy diffusivity function is very sensitive to the slope of the concentration distribution. It was believed that the experimental concentration data near the wall were not satisfactory for the evaluation of the eddy diffusivity function. To circumvent this difficulty, the value of the eddy diffusivity at  $X = 0.95$  was determined as that value which, when combined with the eddy diffusivity profile over the remainder of the column cross section, satisfied the boundary condition,  $R_n(1) = 0$ . In the numerical method used, there was always some residual value of  $R_n(1)$ . Thus, a value of  $R_n(1) \leq 0.0005$  was accepted as being sufficiently near zero.

The series in Equation (7), when applied to turbulent heat transfer, was generally found to converge rapidly and that only the first term in the series was significant (5, 18, 19). It is believed that this may be true only over a limited range of Reynolds numbers for a given  $z/D$  ratio. The assumption that only the first term of the series in Equation (7) is significant is valid only when  $Z$  and hence  $z/D$  is sufficiently large. In this investigation it was found that the second term could not be neglected, as its value was as much as 10% of the magnitude of the first term. This is true because the value of the Reynolds number increases more rapidly than does that of the

eigenvalue. Thus, the exponent  $\lambda_n^2 Z$  decreases as the Reynolds number increases. The net effect is to increase the magnitude of the successive terms of Equation (7).

Because of this fact, the following calculation procedure was employed. The eddy function  $B(X)$  was evaluated from Equation (15) using only the first eigenvalue and eigenfunctions. The eddy function was smoothed and adjusted near the wall to satisfy the boundary conditions as previously described. A value of  $\lambda_2^2$  was then assumed and  $R_2(X)$  was calculated as described in reference 17. An iterative approach determined the value of  $\lambda_2^2$  which resulted in  $R_2(X)$  for which  $R_2(1) = 0$ . The second eigenfunction  $R_2(X)$  was used then to calculate  $C_2$  from Equation (13). All factors in the second term were then known and its value was calculated. This resulted in a function of  $X$ :

$$F(X) = C_2 R_2(X) e^{-\lambda_2^2 Z} \quad (16)$$

Then, the assumption was made that two terms of Equation (7) were adequate to represent  $\theta(X, Z)$ . Thus

$$C_1 R_1(X) e^{-\lambda_1^2 Z} = \theta(X, Z) - F(X) \quad (17)$$

and

$$R_1(X) = \frac{\theta(X, Z) - F(X)}{C_1 e^{-\lambda_1^2 Z}} \quad (18)$$

But, since  $R_n(0) = 1.0$

$$C_1 e^{-\lambda_1^2 Z} = \theta(0, Z) - F(0) \quad (19)$$

Thus, Equation (18) may be rewritten as

$$R_1(X) = \frac{\theta(X, Z) - F(X)}{\theta(0, Z) - F(0)} \quad (20)$$

The first eigenfunction was reevaluated by this method. Then the whole procedure was repeated until all the values became essentially constant.

#### VELOCITY AND CONCENTRATION PROFILES

All velocity and concentration profiles used in this work were determined experimentally. Among the various functions which have been proposed to describe the velocity profile for turbulent flow, that of Hobler (20) is worthy of special note. For the case of laminar flow, the equations proposed by Hobler reduce to the Hagen-Poiseuille equation. Hobler's velocity expression gave good agreement with the experimental velocity profiles for all tests conducted with a Reynolds number of 10,000 or more, except for points very near the wall. A graphical comparison is shown in Figure 2. For lower flow rates, the agreement was not as good. These discrepancies are thought to occur because of two reasons. First, the values of the velocity measured near the wall are subject to the most experimental error because of the difficulty of measuring the velocity without disturbing the flow in this region. Second, evaluation of the Hobler profile requires a value of the Fanning friction factor. This value is ordinarily obtained from pressure drop measurements. However, with the equipment used in this investigation, it was not possible to obtain such measurements. Because of this, the friction factor correlation for wetted-wall columns developed by Kamei and Oishi (21) was used to calculate the friction factor. Their expression is as follows:

$$\frac{f_w}{f_o} = 1 + 3.97 \times 10^{-3} (N_{ReL})^{0.476} (\mu_g/\mu_L)^{-0.271} \quad (21)$$

Because of this, any quantitative comparison of the velocity profiles with that of Hobler may be somewhat misleading.

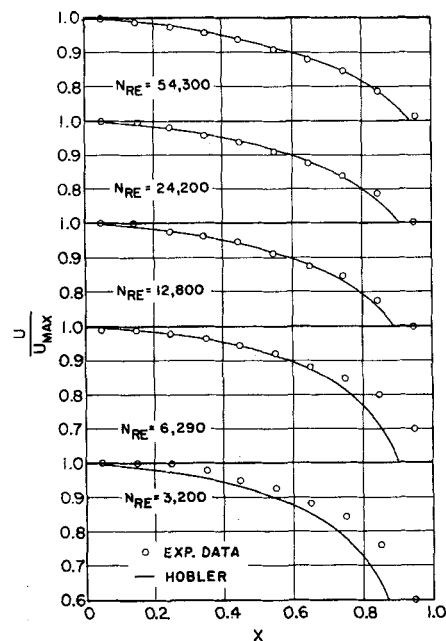


Fig. 2. Experimental velocity profiles.

It may be noted from Figure 2 that there is very little difference between the measured dimensionless velocity profiles for any of the tests. In fact, the Hobler velocity profile evaluated at a Reynolds number of 54,300 approximately fits all velocity data. It is interesting to note that the velocity distribution measured with liquid flowing down the walls was not different from the distribution determined with a dry column within the limits of experimental error. This same result was reported by Schwarz and Hoelscher (4).

The concentration profile data obtained with the use of the lithium chloride probe are plotted in dimensionless form in Figure 3. Two separate tests with the lithium chloride probe were conducted at approximately the same Reynolds number to test the reproducibility of the concentration profile data. The results of these tests are compared in Figure 4. The differences between the curves are believed to be within the limits of reproducibility of the concentration measurements of the probe.

#### DISCUSSION OF RESULTS

The eigenfunctions and the velocity data were smoothed by a five-point orthogonal least squares poly-

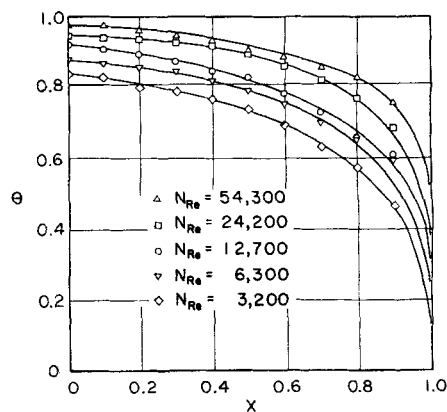


Fig. 3. Experimental concentration profiles.

nomial smoothing formula (22). This step was necessary to calculate reliable derivatives of the eigenfunction for use in Equation (15). After smoothing,  $C_1$  was calculated from Equation (13) with Simpson's rule (23). For purposes of interpolation of the eigenfunction and the velocity function in the application of Simpson's rule, these functions were closely approximated by a polynomial of the type

$$f(X) = A_0 + A_1X^2 + A_2X^4 + \dots + A_nX^{2n} \quad (22)$$

where the constants were determined by a least squares method. The eigenvalue  $\lambda_1^2$  could then be calculated from Equation (14). The numerical differentiation of the eigenfunction was accomplished by a five-point method developed by Whitaker and Pigford (24) and based on Gram orthogonal polynomials.

The eddy mass diffusivity profiles are graphically portrayed in Figure 5. The curves of Figure 5 show striking similarities to those for the eddy viscosity and the eddy thermal diffusivity. At a Reynolds number of 54,300, which corresponded to a high flow rate, it was impossible to prevent serious rippling. While the outline of this curve is similar in appearance to the others, the curve exhibits a sharper and displaced maximum as well as a steeper rise from the wall. The shape of this curve is attributed to this increased turbulence brought about by rippling. Also, the third term in the series of Equation (7) is rapidly becoming significant for the value of  $z/D$  used in this work at this Reynolds number. For this reason, the curve for this flow rate is shown with a dashed line. The greatest uncertainty in the eddy diffusivity profile is near the center ( $X = 0$ ). In this region the slope of the concentration distribution is very small and very slight errors in the concentration are reflected in large changes in the slope. Additional data regarding profiles and eddy values are presented in reference 25.

The numerical solution used to solve the mass diffusion equation utilized the fact that Equation (8) together with its associated boundary conditions is of the Sturm-Liouville type and more particularly that  $R_n(1) = 0$ . This condition can be met only if the vapor pressure at the wall is constant, which in turn is true only if the liquid temperature is constant. Actually it was not possible to maintain the liquid at isothermal conditions in the column due to liquid evaporation. A bulk temperature decrease of from 2° to 4°C. was sometimes observed. To obtain an estimate of the effect this temperature change of the liquid had on the final computed values of the eddy diffusivity, the eddy values were computed for a typical test using two different sets of boundary conditions. In one set, the temperature of the liquid phase was considered constant

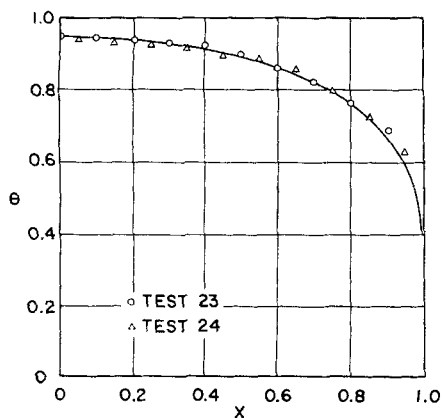


Fig. 4. Reproducibility of concentration measurements.

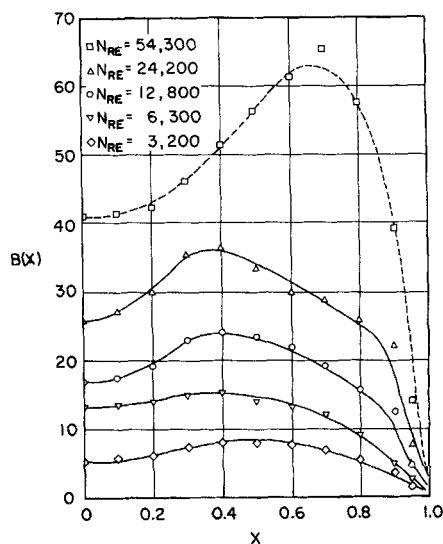


Fig. 5. Dimensionless eddy mass diffusivity profiles.

at its inlet value and in the other set this temperature was considered constant at its outlet value. The test chosen was one in which there was an appreciable change in the temperature and vapor pressure of the liquid phase. The discrepancies between the two sets of data were slight and were well within the uncertainties of the eddy diffusivities. There was, however, some change in the eigenvalues. A more severe test would have been to utilize the liquid surface temperature as a boundary condition. However, this temperature was not available in this particular investigation.

The values of the concentration as calculated from Equation (7) with the computed eddy diffusivity values are in excellent agreement with the experimentally measured values. The uniqueness of the eddy diffusivity function is not assured by the numerical method, but it is of fundamental importance that the function developed is capable of generating the correct concentration distribution.

#### RATIO OF EDDY MASS DIFFUSIVITY TO EDDY VISCOSITY

The relationship between the eddy viscosity and the velocity of a fluid in turbulent flow in a cylindrical duct may be expressed as

$$-\frac{\tau_w g_c r}{\rho R} = (\nu + \nu_E) \frac{du}{dr} \quad (23)$$

with the definition

$$E_M(X) = \frac{\nu + \nu_E}{\nu} \quad (24)$$

Equation (23) can be rearranged to

$$E_M(X) = \frac{-\tau_w X N_{Re} g_c}{2\rho u^2 \frac{dU}{dX}} \quad (25)$$

But

$$f = \frac{2\tau_w g_c}{\rho u^2} \quad (26)$$

Thus

$$E_M(X) = \frac{-f X N_{Re}}{4 \frac{dU}{dX}} \quad (27)$$

An indeterminacy exists at  $X = 0$ , but application of L'Hospital's rule yields

$$E_M(0) = \frac{-fN_{Re}}{4 \frac{d^2U}{dX^2}} \quad (28)$$

As previously pointed out, the Hobler function evaluated for a Reynolds number of 54,300 gave the best fit to the dimensionless experimental velocity data. This function was differentiated and used in Equations (27) and (28). The dimensionless eddy terms  $B(X)$  and  $E_M(X)$  were converted to  $E$  and  $\nu_E$  by their definitions and the ratio  $\gamma$  was defined as

$$\gamma = \frac{E}{\nu_E} = \frac{D_e[B(X) - 1]}{\nu[E_M(X) - 1]} = \frac{B(X) - 1}{N_{Sc}[E_M(X) - 1]} \quad (29)$$

The value of the molecular diffusivity used was that of water in air at the temperature of the gas phase. The ratios of the eddy mass diffusivity and the eddy viscosity can be calculated from Equation (29) for the various Reynolds numbers. Again, the data are more qualitative than quantitative. The individual ratios of the eddy values at various radial positions indicate no trend with the Reynolds numbers employed in this work. However, it does appear that  $\gamma$  is smaller than unity over most of the column cross section, and that the ratio increases rapidly near the center of the duct and shows evidence of increasing again near the wall. The ratio of the eddy mass diffusivity to the eddy viscosity is less than the ratio of the eddy thermal diffusivity to eddy viscosity which was reported by Tao and Strunk (5) to be greater than one for the range of Reynolds numbers used in this investigation. Values of  $\gamma$  averaged over the radial positions  $X = 0.2$  to  $0.8$  were found to be 0.64, 0.80, 0.77, and 0.70 at Reynolds numbers of 3,200, 6,300, 12,800, and 24,200, respectively.

#### NOTATION

$A$	= transfer surface area
$A_n$	= constant [Equation (22)]
$B(X)$	= dimensionless eddy mass diffusivity = $\frac{D_e + E(X)}{D_e}$
$c_a$	= concentration of diffusing material, moles/volume
$C_n$	= constant [Equations (7) and (13)]
$D_{ab}$	= diffusivity of component $a$ through nondiffusing component $b$
$D_v$	= molecular diffusivity, length <sup>2</sup> /time
$E$	= eddy diffusivity, length <sup>2</sup> /time
$E_M(X)$	= dimensionless eddy viscosity = $(\nu + \nu_E)/\nu$
$F(X)$	= function of $X$ , Equation (16)
$f(X)$	= function of $X$ , Equation (22)
$f$	= Fanning friction factor
$f_s$	= friction factor for smooth tubes, Equation (21)
$f_w$	= friction factor for wetted-wall columns, Equation (21)
$g_c$	= conversion factor
$N_a$	= moles of component $a$ transferred per unit time
$N_{Re}$	= Reynolds number
$N_{ReL}$	= Reynolds number of liquid phase
$N_{Sc}$	= Schmidt number
$n$	= order of eigenvalues or eigenfunctions. Also designates $n^{\text{th}}$ term in Equation (22)
$P_a$	= partial pressure of component $a$
$P_a^o$	= vapor pressure of component $a$
$P_i$	= inlet partial pressure of $a$ in $b$
$R$	= radius of column or conduit
$R_n(X)$	= eigenfunction
$R_n'(X)$	= first derivative of eigenfunction
$r$	= radial variable

$U(X)$	= dimensionless velocity = $u(X)/\bar{u}$
$\bar{u}$	= time-smoothed axial velocity
$\frac{u}{\bar{u}}$	= average velocity over cross-sectional area of column
$X$	= dimensionless radial positions = $r/R$
$x$	= length along diffusing path
$Z$	= dimensionless axial length = $z/RN_{Re}N_{Sc}$
$z$	= axial variable

#### Greek Letters

$\Gamma$	= mass flow rate of liquid per unit perimeter
$\gamma$	= ratio of eddy mass diffusivity to eddy viscosity
$\theta$	= dimensionless concentration term = $(P_a^o - P_a)/(P_a^o - P_i)$
$\lambda_n^2$	= eigenvalue
$\mu_g$	= gas phase viscosity
$\mu_L$	= liquid phase viscosity
$\nu$	= kinematic viscosity
$\nu_E$	= eddy viscosity
$\rho$	= density of gas phase
$\tau_w$	= shear stress at the wall

#### LITERATURE CITED

- Boussinesq, T. V., "Mem. Pres. Acad. Sci.," 3 ed., XXIII, 46, Paris (1877) in Bird, R. B., W. E. Stewart, and E. N. Lightfoot, "Transport Phenomena," p. 160, Wiley, New York (1960).
- Isakoff, S. E., and T. B. Drew, "Proceedings of the General Discussion on Heat Transfer," p. 405, Inst. Mech. Engrs. (London) and Am. Soc. Mech. Engrs. (1951).
- Page, F., Jr., W. G. Schlinger, D. K. Breaux, and B. H. Sage, *Ind. Eng. Chem.*, **44**, 424 (1952).
- Schwarz, W. H., and H. E. Hoelscher, *A.I.Ch.E. J.*, **2**, 101 (1956).
- Tao, F. F., Ph.D. dissertation, Univ. Missouri, Rolla (1964).
- Gilliland, E. R., and T. K. Sherwood, *Ind. Eng. Chem.*, **26**, 516 (1934).
- McCarter, R. J., and L. F. Stutzman, *A.I.Ch.E. J.*, **5**, 502 (1959).
- Johnstone, H. F., and R. L. Pigford, *Trans. Am. Inst. Chem. Engrs.*, **37**, 25 (1941).
- Surowiec, A. J., and C. C. Furnas, *ibid.*, **38**, 53 (1942).
- Jackson, M. L., *A.I.Ch.E. J.*, **1**, 229 (1957).
- Thomas, W. J., and S. Portalski, *Ind. Eng. Chem.*, **50**, 1081 (1956).
- Ibid.*, **52**, 1266 (1958).
- Kafesjian, R., C. A. Plank, and E. R. Gerhard, *A.I.Ch.E. J.*, **7**, 463 (1961).
- Emmert, R. E., and R. L. Pigford, *Chem. Eng. Progr.*, **50**, 87 (1954).
- Schrage, K. W., "A Theoretical Study of Interphase Mass Transfer," Columbia Univ. Press, New York (1953).
- Strunk, M. R., M. V. Mitrovic, and D. W. Bunch, *A.I.Ch.E. J.*, **10**, 418 (1964).
- Strunk, M. R., and F. F. Tao, *A.I.Ch.E. J.*, **10**, 269 (1964).
- Sleicher, C. A., Jr., *Trans. Am. Soc. Mech. Engrs.*, **80**, 693 (1958).
- Beckers, H. L., *Appl. Sci. Res.*, **A6**, 147 (1956).
- Hobler, T., *Chem. Stosowana (Poland)*, **1**, 1 (1957).
- Kamei, S., and J. Oishi, *Chem. Eng. (Japan)*, **18**, 421 (1954).
- Hildebrand, F. B., "Introduction to Numerical Analysis," pp. 295-296, McGraw-Hill, New York (1956).
- Ibid.*, p. 73.
- Whitaker, S., and R. L. Pigford, *Ind. Eng. Chem.*, **52**, 185 (1960).
- Bunch, D. W., Ph.D. dissertation, Univ. Missouri, Rolla (1964).

Manuscript received July 28, 1964; revision received July 25, 1965; paper accepted July 28, 1965.